

1 **Resilient hemp shiv aggregates with engineered**  
2 **hygroscopic properties for the building industry**

3 **Atif Hussain\***, Juliana Calabria- Holley, Mike Lawrence, Yunhong Jiang

4 BRE Centre for Innovative Construction Materials, Department of Architecture and Civil  
5 Engineering, University of Bath, Bath BA2 7AY, UK

6 \*Corresponding Author: Atif Hussain ([A.Hussain@bath.edu](mailto:A.Hussain@bath.edu))

7

8 **Abstract**

9 This study focuses on the surface treatment of an extremely hydrophilic natural plant material,  
10 hemp shiv, using a functionalised silica based coating to provide hydrophobicity while retaining  
11 its moisture buffering ability. The chemical composition and physical structure of bio-based  
12 materials results in their extremely hydrophilic behaviour. In this work, a simple one step  
13 coating process was used to enhance the water-repellence of hemp shiv without compromising  
14 its ability to adsorb and release moisture. The coating modified the morphology and surface  
15 roughness of hemp shiv providing a hydrophobic surface having a water contact angle of 118°  
16 and reduced the bulk water absorption by 250% over 24 hours. Mercury intrusion porosimetry  
17 (MIP) showed that the treatment refined the pore size distribution of hemp shiv, reducing the  
18 size of larger pores but not completely blocking the smaller pores thereby allowing hemp shiv  
19 to buffer moisture. Fourier-transform infrared spectroscopy (FTIR) revealed the chemical  
20 composition was modified by the coating, reducing the hydroxyl groups. Hemp shiv aggregates  
21 treated with functionalised silica based coating show potential for the development of robust  
22 lightweight building materials with enhanced hydrophobicity.

23

24 **Keywords:** hemp shiv; bio-based aggregates; hygroscopic; moisture buffering;  
25 hydrophobicity; surface engineering.

26

## 27 **1. Introduction**

28 Bio-based aggregates in the building industry has become popular due to their lower embodied  
29 energy, lower CO<sub>2</sub> emissions and good hygrothermal properties reducing the energy demands  
30 of buildings [1]. Hemp shiv is the woody core obtained from the stem of the hemp (*Cannabis*  
31 *Sativa* L.). Hemp shiv based composites have been actively researched due to their high  
32 moisture buffering and good thermal insulation properties providing a comfortable indoor living  
33 environment [2,3]. The moisture buffering property, absorb and release moisture at dynamic  
34 relative humidity levels, of hemp shiv is associated with its pore structure. Hemp shiv has a dry  
35 bulk density of  $107 \pm 3 \text{ kg/m}^3$  [4] and porosity of 76-78% [5] tending to absorb huge volume of  
36 water when compared with other plant materials [6]. The chemical composition of industrial  
37 hemp shiv are: 44-46% cellulose, 18-27% hemicellulose, 22-28% lignin, 1-6% extractives and  
38 1-2% ash [7,8] . Cellulose forms the main structural part of hemp shiv containing free hydroxyl  
39 groups which are responsible for the extreme hydrophilicity. As a result, hemp shiv based  
40 building composites have extremely long drying times when mixed with lime [9], or they have  
41 poor interfacial adhesion with the polymeric matrix [10]. Moisture sensitivity also results in  
42 microbial growth causing degradation of the aggregate cell wall and deterioration of the  
43 composite durability [11].

44

45 The wetting behaviour of any solid surface is governed by the surface chemical composition  
46 and its geometric structure [12,13]. The interaction between surface roughness and chemistry  
47 is actively researched for improving the hydrophobic properties of plant based materials. One  
48 of the mechanisms to enhance the hydrophobicity of plant based materials involves altering  
49 the chemical composition by blocking the cell wall hydroxyl group. Some of the approaches  
50 include addition of silanes [14,15], acetylation [16] or in situ polymerization [17] that involve  
51 chemical modification of the aggregate cell wall. Other approaches that can enhance surface  
52 roughness and hydrophobicity of the material include sol-gel coatings, plasma treatment or  
53 lithography. The sol-gel technique can be carried at room temperature and it is widely used for  
54 enhancing surface hydrophobicity by depositing coatings with low surface energy and

55 increased roughness [18]. Sol-gel coatings have been used on various bio-based materials for  
56 improving their hydrophobicity [14,19–21] however there is limited knowledge on the impact of  
57 sol-gel coatings on hemp shiv. Sol-gel treatment has also proven to improve the fire resistance  
58 and reduce the flammability of cellulose based materials [22].

59

60 This work focuses on modification of hemp shiv surface using a functionalised silica based  
61 coating to enhance to hydrophobicity of hemp shiv without compromising its moisture buffering  
62 capacity. Our work reports the application of a breathable coating on hemp shiv using a simple  
63 one step process. The objective of this work was to investigate the effect of a hydrophobic  
64 silica coating on the porosity, moisture buffering ability and surface morphology of hemp shiv.

65

## 66 **2. Experimental**

### 67 **2.1 Materials**

68 The hemp shiv aggregates (Figure 1) were received from an agricultural cooperative CAVAC,  
69 France. Tetraethyl orthosilicate (TEOS, 98%), nitric acid (HNO<sub>3</sub>, 70%),  
70 hexadecyltrimethoxysilane (HDTMS, 85%) and absolute ethanol were received from Sigma-  
71 Aldrich.



72

73 *Figure 1. Hemp shiv aggregates used in this study.*

74

## 75 **2.2 Coating preparation**

76 The coating was prepared by hydrolysis and condensation of TEOS in water and ethanol and  
77 nitric acid was added as the catalyst. The coating formulation was 1M of TEOS, 4M water, 4M  
78 ethanol and 0.005M nitric acid. The solution was stirred using a magnetic stirrer for 30 minutes  
79 at 300 rpm and 40 °C. After the preparation of silica formulation, 1 wt. % of HDTMS was added  
80 as the hydrophobic agent and the sol was stirred for another 20 minutes at 300rpm. The pH of  
81 the prepared sol was measured to be 1.92.

82

83 The prepared sol aged in a sealed vial for 48 hours at 20 °C. Hemp shiv aggregates were  
84 immersed in the sol for 10 min and then carefully placed on a Petri dish for drying at room  
85 temperature 20 °C for an hour. The aggregates were then dried at 80 °C for an hour in a  
86 laboratory oven. The treated samples were stored in a sealed vial for further sample  
87 characterisation. The treated samples had an average mass gain of 18% due to the deposition  
88 of the silica coating on the hemp shiv. For calculating the amount of residual water, the treated  
89 samples were vacuum sealed in a glass tube, heated at 150°C overnight and then weighed.  
90 The residual water content was found to be 5 wt. % for coated hemp shiv samples. The silica  
91 glass was prepared by aging the sol in a sealed vial for 48 hours at 20 °C and then placed in  
92 oven at 80 °C for at least 120 hours to undergo dehydration. The gel time of the prepared sol  
93 was 101 days when stored in a sealed vial at 20 °C. The coating formulation and the dipping  
94 time has been reported to deposit uniform crack free coatings on hemp in our recently  
95 published paper [23].

96

## 97 **2.3 Contact Angle Measurements**

98 The determination of water contact angle (WCA) was performed by a contact angle meter (First  
99 Ten Ångstroms USA, FTA200 series) using the static sessile drop method. The WCA readings  
100 were taken for a minimum of 3 different samples. The water droplets used during the test had  
101 a volume of 5µl. The recorded images were analysed by FTA32 Video 2.0 software. The  
102 experiment was performed at room temperature ( $20 \pm 1$  °C).

103

#### 104 **2.4 Water absorption test**

105 Prior to the test, the samples were dried overnight in an oven at 80 °C and then weighed for  
106 recording the initial mass. The samples were placed in beaker containing water and since they  
107 have a density lower than water, the samples floated and only one side of the shiv was in  
108 contact with water. Therefore, the water uptake was mainly due to capillary behaviour. The  
109 readings were taken at frequent intervals for 24 hours, in which the sample was taken out of  
110 water using a tweezer, shaken off to remove any visible surface water and then weighed within  
111 30s. Mass readings were recorded to the nearest 0.1 mg and an average of three readings  
112 from different samples was reported as the final measurement [24,25].

113

#### 114 **2.5 Dynamic vapour sorption**

115 For the analysis of the adsorption-desorption isotherm in response to varying humidity levels,  
116 a dynamic vapour sorption equipment DVS Advantage, SMS, UK was used. The test protocol  
117 was adopted from previous studies [24,26]. The samples weighed around 15 mg and  
118 experiment temperature was maintained at 23 °C. The relative humidity (RH) was increased  
119 in steps from 0-90% and then decreased back to 0%. The actual and target RH, sample mass  
120 and running time were continuously recorded during the experiment.

121

122 The data obtained from the isotherms was used to calculate the moisture content of the  
123 samples at any given RH using the following equations:

$$124 \quad MC = \frac{m_2 - m_1}{m_1} \times 100 \quad (1)$$

$$125 \quad MC_R = \frac{m_2 - m_1}{m_0} \times 100 \quad (2)$$

126 Where MC is the measured equilibrium moisture content of the sample;  $MC_R$  is the reduced  
127 equilibrium moisture content of the sample before coating;  $m_0$  is mass of oven dried uncoated  
128 shiv sample;  $m_1$  is the mass of oven dried coated shiv sample;  $m_2$  is the mass of shiv sample  
129 at any given RH. Three cycles of adsorption-desorption were run for each sample and the  
130 second cycle was reported.

131

## 132 **2.6 Scanning Electron Microscopy**

133 Photomicrographs of the samples were captured using a scanning electron microscope (SEM),  
134 JEOL Corporation - Japan Model JSM-6360 operating at 25 kV. The samples were gold coated  
135 to obtain high magnification of morphology and texture.

136

## 137 **2.7 Surface Roughness**

138 For measurement of sample surface roughness, a 3D optical profilometer, Bruker Nano GmbH  
139 ContourGT-K series, Germany was used in non-contact mode. The area analysed for each  
140 test was 0.25\*0.30 mm<sup>2</sup> and magnification was set to 20X. The data was analysed by Vision  
141 64 software and the surface roughness was calculated. The test was performed for at least 3  
142 different samples and the average value was reported.

143

## 144 **2.8 Fourier transform infrared (FTIR) spectroscopy**

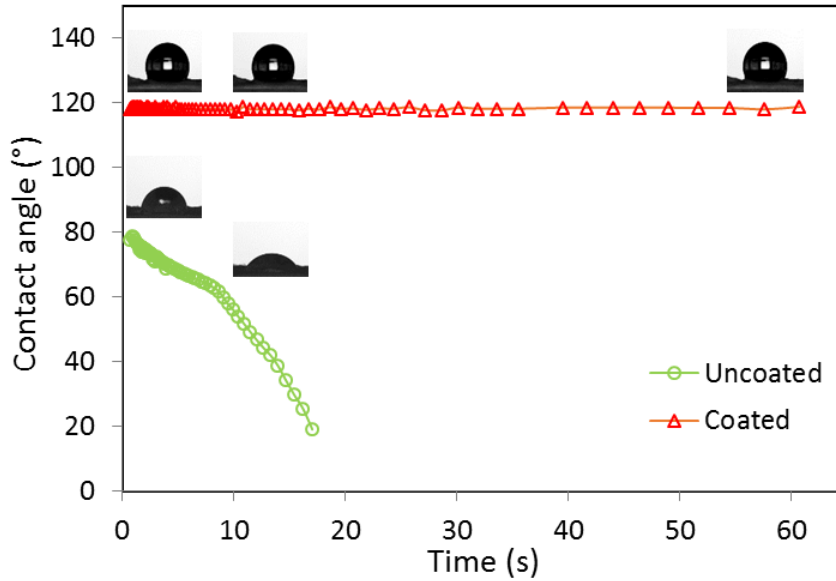
145 For identification of the chemical bonds, FTIR analysis was performed with a PerkinElmer FTIR  
146 spectrometer, Model Frontier. Transmittance spectra were recorded in the range of 4000-600  
147 cm<sup>-1</sup> with a resolution of 2 cm<sup>-1</sup> and 10 scans were run for each test. Hemp shiv samples were  
148 tested as individual pieces whereas the silica glass sample was crushed to powder form and  
149 then mixed with potassium bromide to form pellets.

150

## 151 **3. Results**

152 The water contact angles were recorded from 0-60 seconds of contact between the droplet  
153 and the hemp shiv surface. From Figure 2, it was observed that hemp shiv surface that have  
154 not been coated have highly hydrophilicity. The initial contact angle was 79° and the droplet  
155 sinks into the bulk of the sample completely in less than 20 seconds. On the other hand, the  
156 sol-gel coated samples have an initial contact angle of 118° making the surface hydrophobic.  
157 The contact angle remains stable over 60 seconds of contact.

158



159

160 *Figure 2. Water contact angles of coated and uncoated hemp shiv over time.*

161

162 Water absorption (WA %) measures the relative percentage increase in mass due to the  
 163 retention of water within the bulk of the sample. It is calculated using the following equation:

$$164 \text{ WA \%} = \frac{\text{Sample wet weight} - \text{Sample dry weight}}{\text{Sample dry weight}} \times 100 \quad (3)$$

165

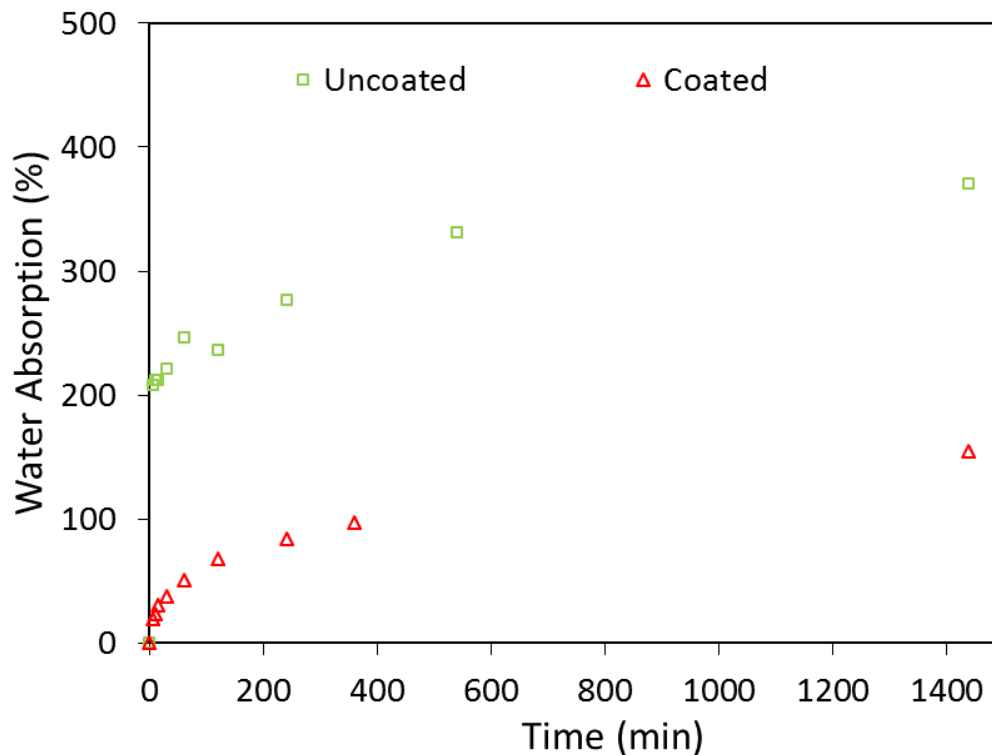
166 Considering the mass increase of hemp shiv due to the coating, equation (3) can be modified  
 167 to calculate the reduced water absorption (WA<sub>R</sub> %) as follows:

$$168 \text{ WA}_R \% = \frac{\text{Coated sample wet weight} - \text{Coated sample dry weight}}{\text{Uncoated sample dry weight}} \times 100 \quad (4)$$

169

170 Figure 3 shows the absorption of water for coated and uncoated hemp shiv samples over 24  
 171 hour period. It was observed that within the initial few minutes of contact with water, hemp shiv  
 172 can absorb a huge volume of water corresponding the significantly high mass increase.  
 173 Uncoated hemp shiv shows extremely high water absorption reaching up to 4 times its initial  
 174 mass after 24 hours. This tendency of absorbing water is mainly caused by the hydrophilic  
 175 behaviour of hemp shiv and its highly porous structure. Hemp shiv treated with the silica  
 176 coating shows a significant reduction in water absorption by almost 250%. The treated shiv  
 177 sample absorbs water only 1.5 times its initial mass over 24 hours. From equation (4), the

178 reduced water absorption of the coated hemp shiv was calculated to be 1.8 times its initial  
179 mass which is still significantly lower than the water absorption of uncoated shiv by 220%.  
180



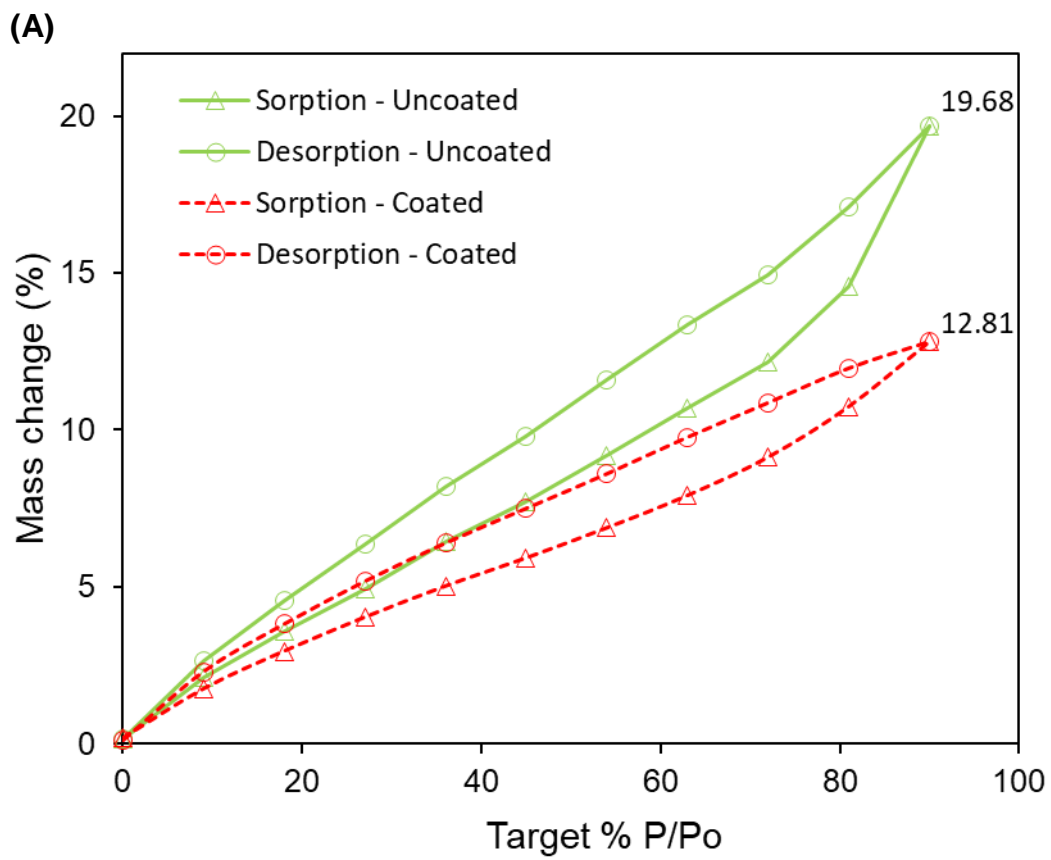
181  
182 *Figure 3. Water absorption of coated and uncoated hemp shiv samples.*

183  
184 The sorption isotherm of coated and uncoated hemp shiv was determined over a RH range 0-  
185 90%. It was observed the coating lowered the measured moisture content (MC) in the  
186 isotherm. The coating decreased the measured MC of the hemp shiv sample by 30%. Coated  
187 shiv showed a maximum measured MC of 12.81% at the highest humidity level of 90%  
188 whereas uncoated hemp shiv had a measured MC value of 19.68 % at 90 % relative humidity  
189 level as seen in Figure 4a. It has been reported that the water molecules were adsorbed on  
190 the surface of hemp shiv linked through hydrogen bonds [27].

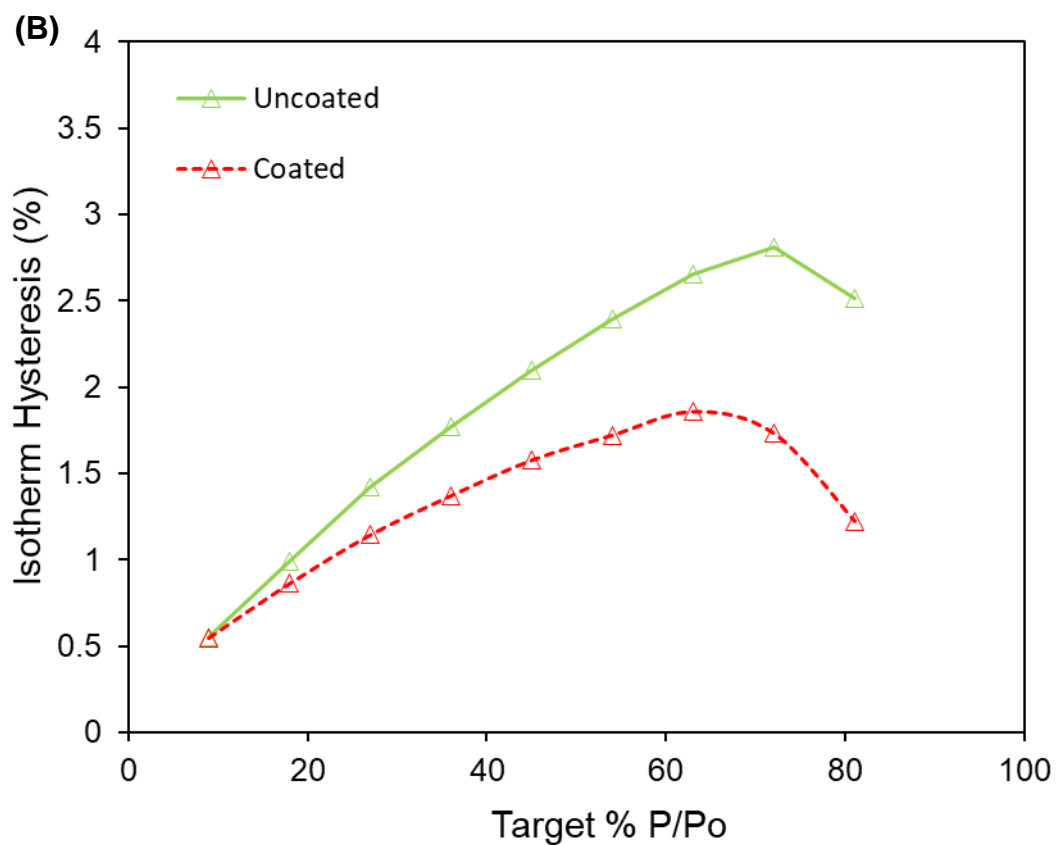
191  
192 It should be noted that the coating increases the mass of hemp shiv and therefore the reduced  
193 moisture content ( $MC_R$ ) of the coated shiv was calculated to be 15.12%. The  $MC_R$  of uncoated  
194 shiv remains the same as its MC which is 19.68% which means that the moisture adsorption  
195 capacity of the coated shiv is not significantly different than the uncoated shiv. The fact that



196 the coating increases the mass of the shiv, equations (1) and (2) show that for uncoated hemp  
197 shiv  $MC = MC_R$  but for coated shiv  $MC < MC_R$  [24,28].  
198



199  
200



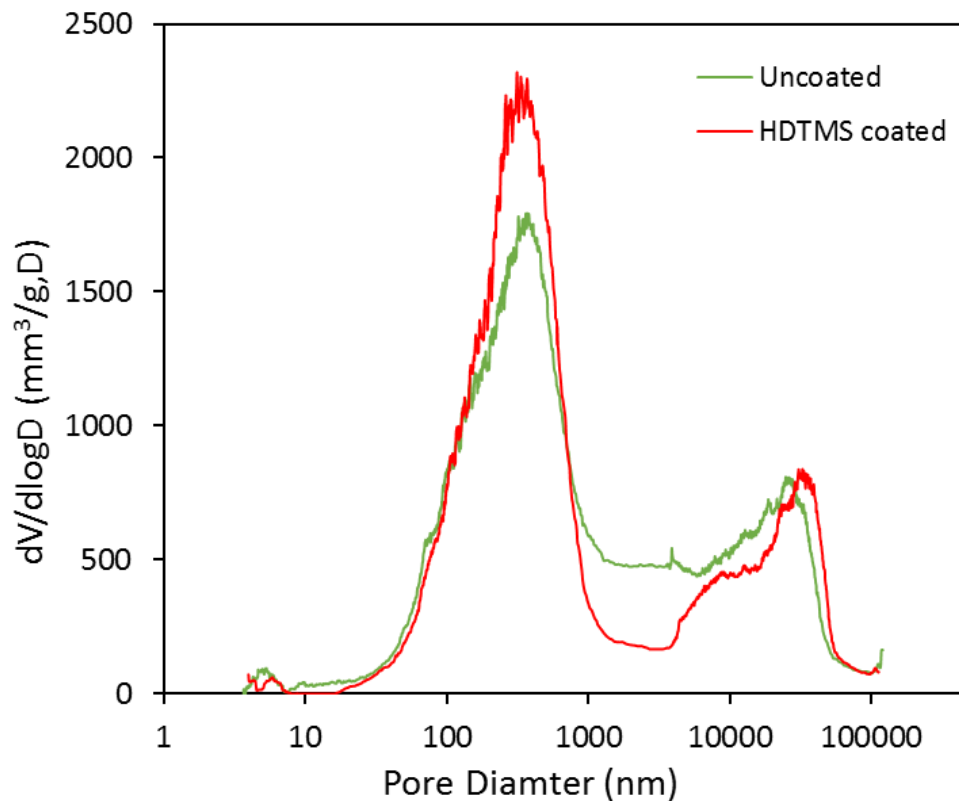
201

202 *Figure 4. (A) Sorption isotherms; (B) isotherm hysteresis curves of uncoated and coated samples.*

203

204 The hysteresis values between adsorption and desorption curves of uncoated and coated shiv  
 205 are presented in Figure 4b. It can be seen from the hysteresis curves that coated shiv shows  
 206 lower hysteresis when compared to uncoated shiv. It was observed that the difference in  
 207 hysteresis between coated and uncoated shiv increased at each higher RH step.

208



209

210 *Figure 5. Pore size distribution of uncoated and coated hemp shiv.*

211

212 The pore size distribution of uncoated and coated shiv is given in Figure 5. The overall porosity  
 213 of hemp shiv is unaffected by the coating and both samples have a porosity of  $78 \pm 0.7\%$ . The  
 214 cumulative pore volume is found to be similar as well,  $2428 \text{ mm}^3/\text{g}$  and  $2377 \text{ mm}^3/\text{g}$  for  
 215 uncoated and coated samples respectively. Figure 5 shows that the coating reduced the  
 216 diameter of the larger pores, mainly in the range of  $1 \mu\text{m}$  to  $10 \mu\text{m}$ . The pores over  $50 \mu\text{m}$   
 217 remain unaffected by the coating suggesting that the layer of coating deposited is very thin  
 218 and in the nanometer scale.

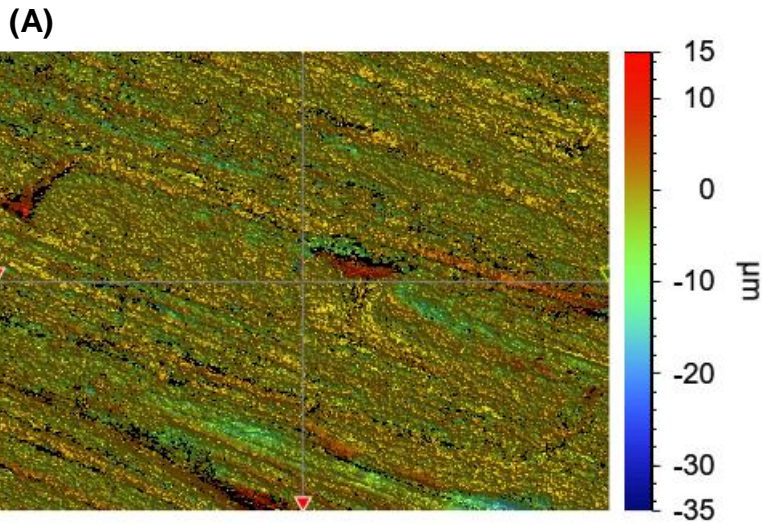
219

220 Another observation from Figure 5 is that the coated shiv has increased number of smaller  
 221 pores in the range of  $100\text{-}800 \text{ nm}$  compared to the uncoated shiv. The overall porosity  
 222 remaining the similar for both samples suggest that the overall pore volume is not reduced but  
 223 only the pores have been refined from micron size to nano size.

224

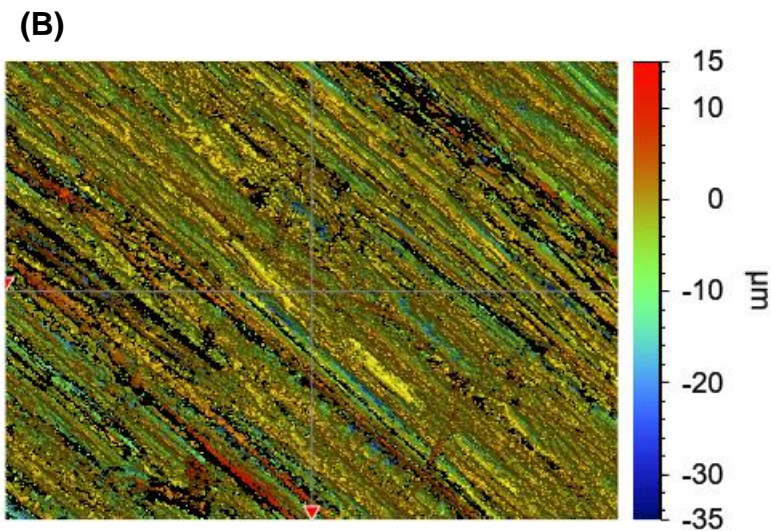
225

226



227

228



229

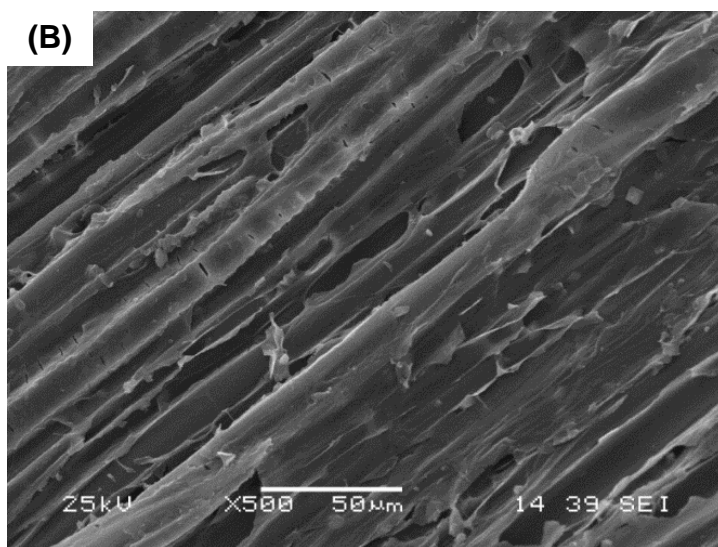
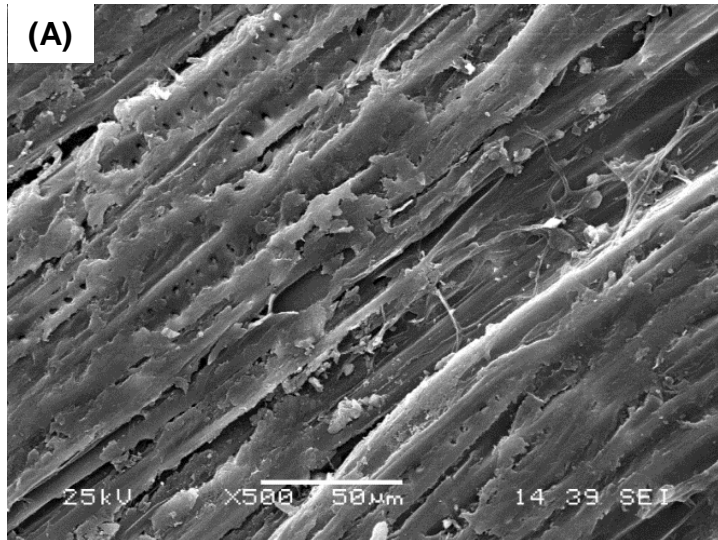
230 *Figure 6. Surface roughness profiles of (a) uncoated; (b) coated shiv.*

231

232 The surface roughness of uncoated and coated hemp shiv samples was analysed by the  
233 software Vision64 and a Robust Gaussian Filter (ISO 16610-31 2016) was applied. The  
234 anatomical influence can be reduced with the help of such filters and the roughness profile can  
235 be optimised for surface evaluation of the sample [29,30]. Moreover, when analysing deep  
236 valleys on the sample surface, the robust Gaussian filter does not produce distortions that  
237 maybe formed by other filters [31]. The mean surface roughness ( $S_a$ ) is the most widely used  
238 parameter for describing the variations in surface height and was calculated according to ISO  
239 4287 (1997). The 3D roughness profile for uncoated and coated hemp shiv surfaces is shown

240 in Figure 6. It was observed that the coating enhanced the surface roughness of the samples  
241 with a mean  $S_a$  value of 2.07  $\mu\text{m}$  compared to uncoated shiv having a mean  $S_a$  value of 1.79  
242  $\mu\text{m}$ .

243

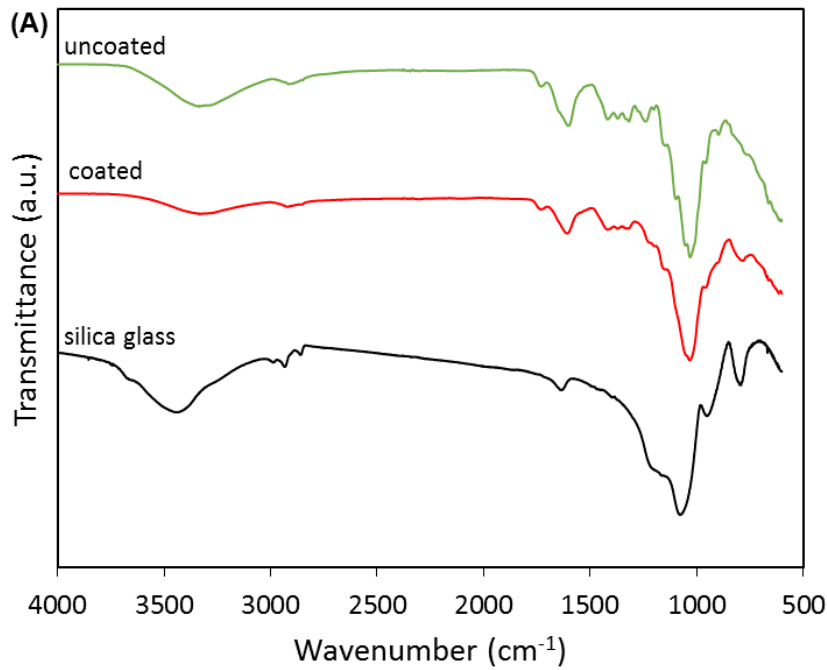


246

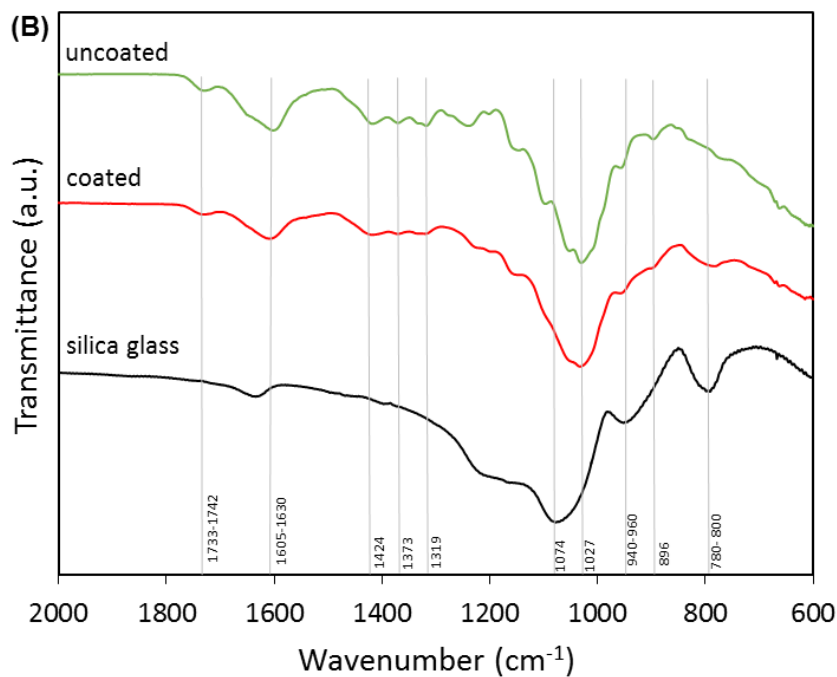
246 *Figure 7. SEM micrographs showing (A) uncoated; (B) coated hemp shiv surface.*

247

248 Morphological characterisation cannot be performed by roughness parameters alone and  
249 therefore microscopic examination is advantageous for better surface evaluations. The surface  
250 morphology of the uncoated and coated surfaces was further evaluated using SEM. From SEM  
251 micrographs in Figure 7, it can be seen that the coating has been uniformly deposited over the  
252 hemp shiv surface without significantly modifying its microstructure.



253



254

255 *Figure 8. FTIR spectra of silica, coated and uncoated shiv samples for (A) 600-4000 cm<sup>-1</sup> region; (B)*  
 256 *600-2000 cm<sup>-1</sup> region.*

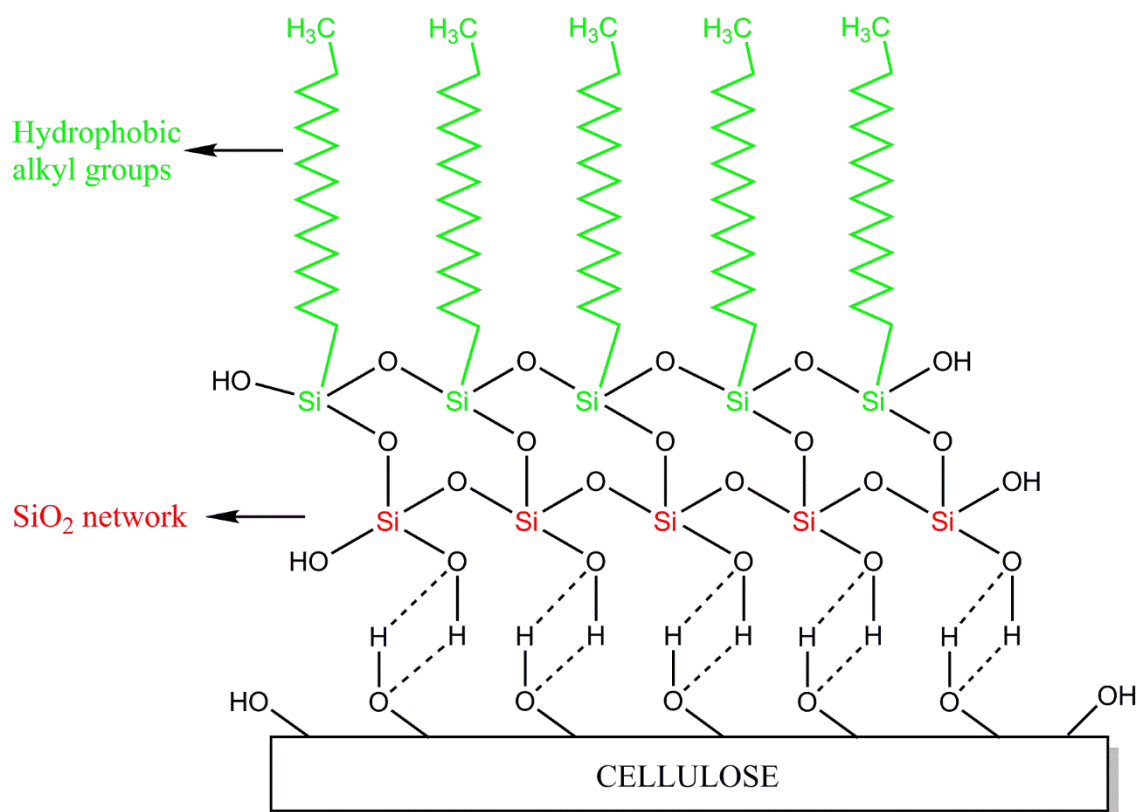
257

258 The FTIR spectra of silica glass, coated and uncoated hemp shiv is shown in Figure 8. Free  
 259 water bands corresponding to the wave number interval 3300-3400 cm<sup>-1</sup> have been reduced in  
 260 the coated shiv samples as seen in Figure 8A. This decrease in signal indicates that the  
 261 hydrophobicity of the shiv has been enhanced by the deposition of the silica coating. The peaks

262 at 2918  $\text{cm}^{-1}$  and 2851  $\text{cm}^{-1}$  correspond to C-H vibration and  $\text{CH}_2$  stretching from  
263 polysaccharides, wax and the alkyl chains. The peaks at wavenumber 1605-1630  $\text{cm}^{-1}$   
264 correspond to adsorbed water. From figure 8B, it was observed that coated shiv showed lower  
265 peak intensity corresponding to wavenumbers 1742-1733  $\text{cm}^{-1}$  (C=O from hemicellulose),  
266 1424  $\text{cm}^{-1}$  ( $\text{CH}_2$ , C=C from cellulose and lignin), 1373  $\text{cm}^{-1}$  (C-H from cellulose), 1319  $\text{cm}^{-1}$  (C-  
267 C,  $\text{CH}_2$  from cellulose and lignin), 1027  $\text{cm}^{-1}$  (C-C, C-OH, C-H from hemicellulose) and 896  $\text{cm}^{-1}$   
268  $^{-1}$  (C-O-C glycosidic bonds from polysaccharides). The deposition of the silica coating can be  
269 confirmed by wavenumbers 940  $\text{cm}^{-1}$  associated with Si-OH bonds vibration and 780  $\text{cm}^{-1}$   
270 incomplete hydrolysis of TEOS molecules. The peak at 1000-1100  $\text{cm}^{-1}$  for the silica glass  
271 corresponds to Si-O-Si bonds.

272

#### 273 4. Discussion



275 *Figure 9. Schematic illustration of sol-gel deposition on hemp shiv surface.*

276

277 The silica based coatings were prepared through the sol-gel process and HDTMS was added  
278 as the hydrophobic agent in the sol formulation. A schematic illustration of deposition of the

279 coating on hemp shiv surface through the hydroxyl sites of cellulose is presented in Figure 9.  
280 During the sol-gel process, hydrolysis and condensation of TEOS forms a silica ( $\text{SiO}_2$ ) network.  
281 The HDTMS molecules self-assemble replacing the hydroxyls on silica network and long alkyl  
282 chains ( $-\text{Si}-\text{C}_{16}$ ) are attached on the silica network. Coating the hemp shiv results in  
283 attachment of the silica network to the shiv surface through the cellulose hydroxyl groups which  
284 are also chemically linked to the alkyl groups responsible for providing hydrophobicity to the  
285 shiv surface.

286

287 The surface wettability of hemp shiv is controlled by the chemical composition and the  
288 morphology. Hemp shiv tends to absorb huge volume of water within a few minutes of contact  
289 as hydroxyl sites are present in large numbers on its surface and in this structure. Moreover,  
290 the extreme hydrophilicity of hemp shiv can also be assigned to its high roughness profile.  
291 Surface roughness can cause an increase or decrease in the water contact angle depending  
292 on the nature of the material. Roughness is defined as the ratio between the actual surface  
293 area to the geometrically projected area. Higher surface roughness results in increased  
294 hydrophilicity for hydrophilic materials but for hydrophobic surfaces, higher surface roughness  
295 enhances the hydrophobicity of the material. For a hydrophilic surface, high surface roughness  
296 provides a large surface area increasing the interaction with a water droplet, thereby providing  
297 a low water contact angle. On the other hand, a hydrophobic surface has micro scale  
298 protrusions which cannot be filled by the liquid and instead filled by air resulting in higher  
299 contact angles [32]. In the present work, the hydrophobicity of the coated hemp shiv surface is  
300 due to the self-assembled layer of HDTMS on the silica network reducing the cellulose hydroxyl  
301 sites as seen in Figure 9. The surface roughness of the hemp shiv was enhanced due the  
302 deposition of the coating. The coated hemp shiv exhibited excellent hydrophobicity with WCA  
303 up to  $118^\circ$  due to the combination of enhanced surface roughness and low surface energy of  
304 the HDTMS chains. Durability studies on composites made with treated hemp shiv by  
305 completely immersing them in water for 24 hours and testing their mechanical performance  
306 have been reported in a recent paper [33].

307



308 The microstructure of hemp shiv remained unaltered after sol-gel treatment. From SEM results,  
309 it was observed that the coating was deposited as a uniform layer and no cracks were observed  
310 after drying the shiv. The hydrophobicity of the substrate can be affected by cracks in the  
311 coating layer as water molecules can penetrate, wetting the substrate over time. The water  
312 absorption results showed that the sol-gel coating layer provided excellent resistance to water  
313 due to the hydrophobic functional groups in the coating. The water uptake for the coated hemp  
314 shiv was massively reduced within the first few minutes of contact and the water absorption  
315 was reduced by 250% over 24 hours when compared to the uncoated shiv.

316

317 The high values of moisture adsorption for hemp shiv can be assigned to its chemical  
318 composition with a large number of hydroxyl groups being accessible. The lower water vapour  
319 sorption values for the coated shiv can be attributed to the hydrophobic alkyl chains present  
320 on the coated surface. Modifying the surface of hemp shiv with the silica coating blocked the  
321 surface hydroxyl sites and reduced the mass of water adsorbed at high humidity levels. The  
322 silica coating interacts with the hemp shiv subsequently lowering its moisture buffering capacity  
323 to a limited extent but the coating does not completely block the pores. This is also in  
324 agreement with the SEM micrographs showing this coating formulation had least altered the  
325 surface morphology of hemp shiv. From the porosity and DVS results, it can be determined  
326 that the coated hemp shiv is capable of adsorbing moisture through the smaller pores whereas  
327 the water uptake is considerably reduced due to decrease in the larger pores. Coated shiv  
328 showed significant reduction in hysteresis by 49% when compared to uncoated shiv at 90%  
329 RH. The reduction in hysteresis curves of the coated shiv shows that water is condensed only  
330 on the surface and does not go further deep into the bulk of the hemp shiv structure due to the  
331 presence of hydrophobic chains.

332

## 333 **5. Conclusions**

334 Sol-gel technology has been successfully applied for surface modification of hemp shiv  
335 enhancing its hydrophobicity while retaining its moisture buffering capacity. A simple one step

336 coating process has been used to provide a hydrophobicity to a highly hydrophilic bio-based  
337 material. The coated surface exhibited excellent hydrophobic properties through the  
338 synergistic effect of enhanced surface roughness and modified chemical composition. Uniform  
339 crack-free monolayer surface coatings delivered contact angles up to 118° and significantly  
340 lowered the water absorption rate. The sol-gel coating does not significantly alter the  
341 microstructure of the shiv thereby retaining the ability to adsorb and desorb humidity. Silica  
342 coated hemp shiv has the potential to be used as a superior aggregate and mixed with binders  
343 to produce water-resistant bio-based building composites.

344

### 345 **Funding**

346 The work was supported by the ISOBIO project funded by the Horizon 2020 programme [Grant  
347 number 636835 – ISOBIO – H2020-EeB-2014-2015] and the EPSRC Centre for  
348 Decarbonisation of the Built Environment (dCarb) [grant number EP/L016869/1]. The contents  
349 of this publication are the sole responsibility of the authors and can in no way be taken to reflect  
350 the views of the European Union.

351

### 352 **Acknowledgments**

353 The authors thank Prof Pierre Blanchet and Dr Diane Schorr for access to 3D profilometer at  
354 Université Laval.

355

### 356 **Data access statement**

357 All data are provided in full in the results section of this paper.

358

### 359 **Disclosure statement**

360 The authors declare that they have no conflict of interest.

361

### 362 **References**

363 [1] M. Lawrence, Reducing the Environmental Impact of Construction by Using  
364 Renewable Materials, *J. Renew. Mater.* 3 (2015) 163–174.

- 365 doi:10.7569/JRM.2015.634105.
- 366 [2] E. Latif, M. Lawrence, A. Shea, P. Walker, Moisture buffer potential of experimental  
367 wall assemblies incorporating formulated hemp-lime, *Build. Environ.* 93 (2015) 199–  
368 209. doi:10.1016/j.buildenv.2015.07.011.
- 369 [3] F. Collet, J. Chamoin, S. Pretot, C. Lanos, Comparison of the hygric behaviour of  
370 three hemp concretes, *Energy Build.* 62 (2013) 294–303.  
371 doi:10.1016/j.enbuild.2013.03.010.
- 372 [4] B. Mazhoud, F. Collet, S. Pretot, C. Lanos, Mechanical properties of hemp-clay and  
373 hemp stabilized clay composites, *Constr. Build. Mater.* 155 (2017) 1126–1137.  
374 doi:10.1016/j.conbuildmat.2017.08.121.
- 375 [5] Y. Jiang, M. Lawrence, M.P. Ansell, A. Hussain, Cell wall microstructure, pore size  
376 distribution and absolute density of hemp shiv, *R. Soc. Open Sci.* 5 (2018) 171945.  
377 doi:10.1098/rsos.171945.
- 378 [6] H.R. Kymainen, M. Hautala, R. Kuisma, A. Pasila, Capillarity of flax/linseed (*Linum*  
379 *usitatissimum* L.) and fibre hemp (*Cannabis sativa* L.) straw fractions, *Ind. Crops Prod.*  
380 14 (2001) 41–50. doi:10.1016/S0926-6690(00)00087-X.
- 381 [7] L. Kidalova, N. Stevulova, E. Terpakova, Influence of water absorption on the selected  
382 properties of hemp hurds composites, *Pollack Period.* (2015).  
383 doi:10.1556/Pollack.10.2015.1.12.
- 384 [8] M.R. Vignon, D. Dupeyre, Steam explosion of woody hemp ch nevotte, 17 (1995)  
385 395–404.
- 386 [9] L. Arnaud, E. Gourlay, Experimental study of parameters influencing mechanical  
387 properties of hemp concretes, *Constr. Build. Mater.* 28 (2012) 50–56.  
388 doi:10.1016/j.conbuildmat.2011.07.052.
- 389 [10] J. Gassan, V.S. Gutowski, A.K. Bledzki, About the surface characteristics of natural  
390 fibres, *Surf. Eng.* 283 (2000) 132–139. doi:10.1002/1439-  
391 2054(20001101)283:1<132::AID-MAME132>3.0.CO;2-B.
- 392 [11] S. Marceau, P. Glé, M. Guéguen-Minerbe, E. Gourlay, S. Moscardelli, I. Nour, S.  
393 Amziane, Influence of accelerated aging on the properties of hemp concretes, *Constr.*  
394 *Build. Mater.* 139 (2017) 524–530. doi:10.1016/j.conbuildmat.2016.11.129.
- 395 [12] J. Genzer, K. Efimenko, Recent developments in superhydrophobic surfaces and their  
396 relevance to marine fouling: a review., *Biofouling.* 22 (2006) 339–360.  
397 doi:10.1080/08927010600980223.
- 398 [13] A. Nakajima, K. Hashimoto, T. Watanabe, Recent studies on super-hydrophobic films,  
399 in: *Monatshefte Fur Chemie*, 2001: pp. 31–41. doi:10.1007/s007060170142.
- 400 [14] S. Donath, H. Militz, C. Mai, Wood modification with alkoxysilanes, *Wood Sci. Technol.*  
401 38 (2004) 555–566. doi:10.1007/s00226-004-0257-1.
- 402 [15] U. Benitha Sandrine, V. Isabelle, M. Ton Hoang, C. Maalouf, Influence of chemical  
403 modification on hemp-starch concrete, *Constr. Build. Mater.* 81 (2015) 208–215.  
404 doi:10.1016/j.conbuildmat.2015.02.045.
- 405 [16] M.M. Kabir, H. Wang, K.T. Lau, F. Cardona, Chemical treatments on plant-based  
406 natural fibre reinforced polymer composites: An overview, *Compos. Part B Eng.* 43  
407 (2012) 2883–2892. doi:10.1016/j.compositesb.2012.04.053.

- 408 [17] E. Cabane, T. Keplinger, V. Merk, P. Hass, I. Burgert, Renewable and functional wood  
409 materials by grafting polymerization within cell walls, *ChemSusChem*. 7 (2014) 1020–  
410 1025. doi:10.1002/cssc.201301107.
- 411 [18] J. Song, O.J. Rojas, Approaching super-hydrophobicity from cellulosic materials : A  
412 Review, *Pap. Chem.* 28 (2013) 216–238. doi:10.3183/NPPRJ-2013-28-02-p216-238.
- 413 [19] S. Wang, C. Liu, G. Liu, M. Zhang, J. Li, C. Wang, Fabrication of superhydrophobic  
414 wood surface by a sol-gel process, *Appl. Surf. Sci.* 258 (2011) 806–810.  
415 doi:10.1016/j.apsusc.2011.08.100.
- 416 [20] B. Mahltig, H. Böttcher, Modified silica sol coatings for water-repellent textiles, *J. Sol-  
417 Gel Sci. Technol.* 27 (2003) 43–52. doi:10.1023/A:1022627926243.
- 418 [21] G.Y. Bae, B.G. Min, Y.G. Jeong, S.C. Lee, J.H. Jang, G.H. Koo, Superhydrophobicity  
419 of cotton fabrics treated with silica nanoparticles and water-repellent agent, *J. Colloid  
420 Interface Sci.* 337 (2009) 170–175. doi:10.1016/j.jcis.2009.04.066.
- 421 [22] J. Mastalska-Popławska, M. Pernechele, T. Troczynski, P. Izak, Thermal properties of  
422 silica-coated cellulose fibers for increased fire-resistance, *J. Sol-Gel Sci. Technol.* 83  
423 (2017) 683–691. doi:10.1007/s10971-017-4445-5.
- 424 [23] A. Hussain, J. Calabria-Holley, D. Schorr, Y. Jiang, M. Lawrence, P. Blanchet,  
425 Hydrophobicity of hemp shiv treated with sol-gel coatings, *Appl. Surf. Sci.* 434 (2018)  
426 850–860. doi:10.1016/j.apsusc.2017.10.210.
- 427 [24] A. Hussain, J. Calabria-Holley, Y. Jiang, M. Lawrence, Modification of hemp shiv  
428 properties using water-repellent sol–gel coatings, *J. Sol-Gel Sci. Technol.* 86 (2018)  
429 187–197. doi:10.1007/s10971-018-4621-2.
- 430 [25] Y. Jiang, M.A. Bourebrab, N. Sid, A. Taylor, F. Collet, S. Pretot, A. Hussain, M. Ansell,  
431 M. Lawrence, Improvement of Water Resistance of Hemp Woody Substrates through  
432 Deposition of Functionalized Silica Hydrophobic Coating, while Retaining Excellent  
433 Moisture Buffering Properties, *ACS Sustain. Chem. Eng.* 6 (2018) 10151–10161.  
434 doi:10.1021/acssuschemeng.8b01475.
- 435 [26] C.A.S. Hill, A. Norton, G. Newman, The water vapor sorption behavior of natural  
436 fibers, *J. Appl. Polym. Sci.* (2009). doi:10.1002/app.29725.
- 437 [27] Y. Jiang, M. Lawrence, A. Hussain, M. Ansell, P. Walker, Comparative moisture and  
438 heat sorption properties of fibre and shiv derived from hemp and flax, *Cellulose*. 0  
439 (2018). doi:10.1007/s10570-018-2145-0.
- 440 [28] Y. Xie, C.A.S. Hill, Z. Xiao, H. Militz, C. Mai, Silane coupling agents used for natural  
441 fiber/polymer composites: A review, *Compos. Part A Appl. Sci. Manuf.* 41 (2010) 806–  
442 819. doi:10.1016/j.compositesa.2010.03.005.
- 443 [29] Y. Fujiwara, Y. Fujii, Y. Sawada, S. Okumura, Assessment of wood surface  
444 roughness: Comparison of tactile roughness and three-dimensional parameters  
445 derived using a robust Gaussian regression filter, *J. Wood Sci.* 50 (2004) 35–40.  
446 doi:10.1007/s10086-003-0529-7.
- 447 [30] L. Gurau, H. Mansfield-Williams, M. Irle, Filtering the roughness of a sanded wood  
448 surface, *Holz Als Roh - Und Werkst.* 64 (2006) 363–371. doi:10.1007/s00107-005-  
449 0089-1.
- 450 [31] B. Ugulino, R.E. Hernández, Assessment of surface properties and solvent-borne

- 451 coating performance of red oak wood produced by peripheral planing, *Eur. J. Wood*  
452 *Wood Prod.* (2016) 1–13. doi:10.1007/s00107-016-1090-6.
- 453 [32] H. Teisala, M. Tuominen, J. Kuusipalo, Superhydrophobic Coatings on Cellulose-  
454 Based Materials: Fabrication, Properties, and Applications, *Adv. Mater. Interfaces.* 1  
455 (2014) 1–20. doi:10.1002/admi.201300026.
- 456 [33] A. Hussain, J. Calabria-Holley, M. Lawrence, M.P. Ansell, Y. Jiang, D. Schorr, P.  
457 Blanchet, Development of novel building composites based on hemp and multi-  
458 functional silica matrix, *Compos. Part B Eng.* 156 (2018) 266–273.  
459 doi:10.1016/J.COMPOSITESB.2018.08.093.
- 460